Formation of Amyloid Fibrils via Longitudinal Growth of Oligomers†

Puja Shahi,‡ Ritu Sharma, Shefali Sanger, Ish Kumar,§ and Ravinder S. Jolly*

Institute of Microbial Technology, Sector 39, Chandigarh 160 036, India

Received January 19, 2007; Revised Manuscript Received April 23, 2007

ABSTRACT: Mature amyloid fibrils are believed to be formed by the lateral association of discrete structural units designated as protofibrils, but this lateral association of protofibrils has never been directly observed. We have recently characterized a thioesterase from *Alcaligenes faecalis*, which was shown to exist as homomeric oligomers with an average diameter of 21.6 nm consisting of 22 kDa subunits in predominantly β-sheet structure. In this study, we have shown that upon incubation in a 75% ethanol solution, the oligomeric particles of protein were transformed into amyloid-like fibrils. TEM pictures obtained at various stages during fibril growth helped us to understand to a certain extent the early events in the fibrillization process. When incubated in 75% ethanol, oligomeric particles of protein grew to ∼35−40 nm in diameter before fusion. Fusion of two oligomers of 35−40 nm resulted in the formation of a fibril. Fibril formation was accompanied by a reduction in the diameter of the particle to ∼20−25 nm along with concomitant elongation to ∼110 nm, indicating reorganization and strengthening of the structure. The elongation process continued by sequential addition of oligomeric units to give fibers 500−1000 nm in length with a further reduction in diameter to 17−20 nm. Further elongation resulted in the formation of fibers that were more than 4000 nm in length; the diameter, however, remained constant at 17−20 nm. These data clearly show that the mature fibrils have assembled via longitudinal growth of oligomers and not via lateral association of protofibrils.

The formation of well-ordered amyloid fibrils by the self-assembly of various proteins and polypeptides is associated with various human medical disorders like Alzheimer's disease, polyglutamine (poly-Q),[1] Parkinson's diseases, Huntington's diseases, encephalopathies and cystic fibrosis, the gelsolin amyloid disease, prion disorders (bovine spongiform encephalopathy and Creutzfeldt-Jakob disease), type II diabetes, and many others. Currently, ∼20 different known syndromes are associated with the formation of amyloid deposits (*1*−*4*). The formation of amyloid fibrils from proteins and peptides appears to be a common phenomenon. It has been suggested that most if not all proteins have the ability to form amyloid fibrils under certain conditions. The formation of typical amyloid fibrils has been reported from several disease-unrelated proteins (*1*, *5*−*7*). Moreover, the amyloid formation as a natural evolution mechanism has been shown recently on the basis of the results of studies which point to the involvement of self-assembled amyloid fibrils in the formation of biofilm and aerial hyphae by microorganisms (*8*−*10*).

Understanding the molecular basis of amyloid disease requires an understanding of the mechanism by which normally soluble protein is transformed into a fibrillar form. The polymorphic aspects of the mature fibrils have been well characterized, but the studies investigating the assembly process remain limited. Fibrillogenesis processes require a critical protein concentration and formation of a discrete, structured intermediate designated as the amyloid protofibril (*11*−*13*). The protofibril was proposed as a building block of the thicker higher-order mature fibrils, which were thought to form by lateral association of protofibrils (*11*, *14*), but this lateral association of protofibrils has never been directly observed. Atomic force microscopy (AFM) data, recently described by Green et al. (*15*), suggest that the mature fibrils from human amylin (hA) are unlikely to be assembled by the lateral association of protofibrils.

Recently, we have reported the characterization of a novel thioesterase from *Alcaligenes faecalis* MTCC 7733 (*16*, *17*). In solution, the protein existed as oligomers 21.6 nm in average diameter consisting of 22 kDa subunits. CD spectra of the aggregated protein revealed features characteristic of β-sheet structure. We have been able to identify solution conditions for the transformation of these oligomeric units into amyloid-like fibrils. TEM micrographs obtained at various stages during growth of amyloid at a protein concentration of 2.3 μM helped us to understand to a certain extent the early events in the fibrillization process. Our observations suggested that for this protein the matured fibrils have assembled directly via longitudinal growth of oligomers

† This work was supported by a grant from the Council of Scientific and Industrial Research, New Delhi, and by research fellowships to P.S., S.S., R.S., and I.K.

* To whom correspondence should be addressed: Institute of Microbial Technology, Sector 39, Chandigarh 160 036, India. Phone: 91-172-226-3680. Fax: 91-172-269-0132. E-mail: jolly@imtech.res.in.

‡ Present address: Department of Physiology and Biophysics, University of Iowa, Iowa City, IA 52242.

§ Present address: Department of Chemistry, Wesleyan University, Middletown, CT 06459.

[1] Abbreviations: TEM, transmission electron microscopy; AD, Alzheimer's disease; poly-Q, polyglutamine; hA, human amylin; PI3-SH3, SH3 domain of phosphatidylinositol 3′-kinase; CD, circular dichroism; TFE, trifluoroethanol; CR, Congo red; ThT, thioflavin T; DTNB, 5,5′-dithiobis(2-nitrobenzoic acid); UA, uranyl acetate; PTA, phosphotungstic acid.

10.1021/bi7001136 CCC: $37.00
Published on Web 05/31/2007

in a nucleation-dependent polymerization process. Under the solution conditions that were used, no lateral association of protofibrils was observed in this case. These observations become significant when considered in light of a recent study that has shown that overt neuronal cell death mediated by Aβ1−40 was critically dependent on ongoing Aβ1−40 nucleation-dependent polymerization, which in turn was dependent on the concentration of both soluble and fibrillar Aβ. The neurotoxic potency of Aβ increased as the number of fibril ends increased, which would be expected for a nucleation-dependent polymerization process (*18*). Since the pathogenecity of protein deposition diseases has been shown to be directly related to the structural nature of the aggregates rather than the specific sequence of the proteins from which they arise, thioesterase of bacterial origin, not associated with any disease condition, possibly can be used as a model for studying the molecular basis of amyloid diseases (*19*).

MATERIALS AND METHODS

Bacterial Strain. A. faecalis MTCC 7733 (http://mtcc.imtech.res.in/cgi-bin/mainhit.pl) was used in this study.

Extraction and Purification of Thioesterase. Extraction and purification of thioesterase were carried out as described previously (*16*). Briefly, *A. faecalis* was grown at 37 °C to an absorbance at 600 nm (A_{600}) of 4.0 in a rich medium with peptone (1%) and beef extract (0.5%). The cell pellet corresponding to 2 L of culture was washed with 50 mM phosphate buffer (pH 7.0) and suspended in the same buffer containing 1 M NaCl at a concentration of 2 g (wet mass)/mL. The cell suspension was incubated at 37 °C for 2 h with shaking at 200 rpm. The cells were removed by centrifugation at 16000*g* for 30 min. Sepharose 4B (fractionation range of 60−20000 kDa) 13 mm × 290 mm gel filtration columns were used for protein purification. The individual fractions were assayed for their activity by the DTNB method, as described below. The active fractions were pooled together and concentrated by ultrafiltration using a 50 kDa membrane (Amicon).

Assay Methods for Thioesterase Activity. Thioesterase activity was measured by following the increase in absorbance at A_{412} ($\epsilon = 13\,600\ M^{-1}\ cm^{-1}$) when free thiol formed during deacylation of acyl-CoA reacted with DTNB as previously described (*20*). Each assay mixture contained 100 mM Tris-HCl buffer (pH 7.6), 0.4 mM DTNB, and 100 μM stearoyl-CoA in a final volume of 0.5 mL. The reaction was started by addition of an aliquot of thioesterase (0.2 μg) followed by incubation at 25 °C. The change in absorption was recorded at 412 nm after 30 s and 1, 2, 3, and 4 min.

Solution Conditions for the Growth of Fibrils. A fresh sample of purified thioesterase was concentrated to 200 μg/mL by ultracentrifugation using a 50 kDa Centricon membrane. Samples were prepared by adding 50 μL of this protein to 150 μL of assay buffer [50 mM phosphate buffer (pH 7.4)] as a control or to 150 μL of ethanol (final concentration of 75%) as a test sample and incubated at 25 °C for the specified period of time. Aliquots of control and test samples were withdrawn at 24 h intervals and tested for amyloid formation by the following methods.

Congo Red Binding. Samples were tested for amyloid fibril−Congo red (CR) binding by the spectroscopic bandshift assay (*21*). A fresh CR solution was prepared by dissolving the dye in assay buffer at a concentration of 415 μM and filtering it three times with a 0.22 μm filters. For the assay, absorption spectra of 1 mL of assay buffer [5 mM phosphate buffer (pH 7.4) and 0.15 mM NaCl] containing 12 μL of a solution of dye (at a final concentration of ∼5 μM) were recorded from 400 to 600 nm after the addition of 75 μL of protein samples. The reaction samples were thoroughly mixed and incubated at room temperature for 15 min before the absorbance was recorded. Protein sample alone and CR dye alone in assay buffer were used as controls.

Congo Red Birefringence. A 20 μL aliquot of the protein sample was placed on microscopic slides and left in air for drying for 15−20 min, and 10 μL of 1% NaOH was added to 1 mL of a stock solution of 80% ethanol in 5 mM phosphate buffer (pH 7.4) saturated with Congo red and sodium chloride, as described previously (*22*). An alkaline solution was applied to slides for 2 min and then poured off; the slides were then rinsed with several portions of 80% ethanol in 5 mM phosphate buffer (pH 7.4). Stained sections were air-dried overnight and visualized at a magnification of 40×. Birefringence was observed between cross polarizers.

Thioflavin T Fluorescence. A fresh thioflavin T (ThT M_r = 318) solution at a concentration of 2.5 mM was prepared in assay buffer [5 mM phosphate buffer (pH 7.4) and 0.15 mM NaCl], and 10 μL of this was added to 100 μL of protein sample and 890 μL assay buffer just before the fluorescence was recorded, as described previously (*23*). The spectra were recorded in a Perkin-Elmer luminescence spectrometer (LS50B) using a quartz cell with a light path of 10 mm. The excitation wavelength was set at 440 nm; emission was recorded at 485 nm, or a spectrum was taken from 400 to 600 nm to record the absorbance maxima. Thioflavin T alone was used as a control in these experiments.

Circular Dichroism Analysis. Protein samples were incubated at room temperature for the indicated times and aliquots withdrawn at definite time intervals. Stock solutions of both control and test samples were centrifuged at 14 000 rpm for 10 min. Samples for CD analysis were prepared by diluting these in filter-sterilized (0.22 μm filters) 50 mM sodium phosphate buffer (pH 7.2) to a final concentration of 15 μg/mL. These were then transferred to a quartz cell with a path length of 0.2 cm. Spectra were acquired using a Jasco (Easton, MD) J-715 spectrophotometer at 23 °C. The CD spectra were collected from 200 to 250 nm with a response time of 0.25 s, a scan speed of 50 nm/min, a resolution of 1.0 nm, and five cumulative scans. Secondary structures were estimated from the spectra using a principal component regression analysis method. All CD spectra are given comparing raw ellipticities of various samples.

Electron Microscopy. Protein was analyzed for fibril formation by negative staining. The samples were absorbed for 4−5 min on carbon-coated 600-mesh copper grids, stained with freshly filtered 2% UA (w/v) and 2% PTA (w/v) (pH 7.5). These were then viewed in a JEOL (Tokyo, Japan) 1200CXII transmission electron microscope. Random fields were photographed at 80 kV with magnification ranging from 25000× to 80000×.

Seeding Experiments. Thioesterase (50 μg/mL) in 75% ethanol (v/v) was incubated for 8 days at room temperature, and 100 μL of this ethanol-induced seeding solution was added to freshly prepared solution of thioesterase in 75% ethanol at a concentration of 50 μg/mL. These experiments

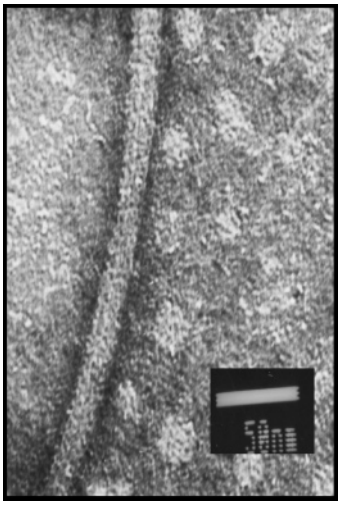

FIGURE 1: Transmission electron micrographs. Purified protein at ~9 μM in phosphate buffer (pH 7.0) was incubated at room temperature for 7 days and examined by transmission electron microscopy (TEM) for formation of any fibrils.

were carried out with appropriate controls. The first control involved the incubation of an identical solution of thioesterase in the absence of the aliquot of seeding solution, and the second control involved dilution of an approximate aliquot of the seeding solution into phosphate buffer. The aggregation was monitored via a CR binding assay, ThT fluorescence, CD spectroscopy, and transmission electron microscopy.

RESULTS

Characterization of Fibrils. Protein used in this study is a novel thioesterase from *A. faecalis* recently characterized by us (*16*, *17*). The fresh sample of purified thioesterase obtained by size exclusion chromatography over a Sephadex 4B column was concentrated by repeated ultrafiltration using a Centricon 50 kDa membrane, suspended in water at concentration of 600 μg/mL, and subjected to TEM. The electron micrograph showed the protein as granular micellelike structures having an average diameter of 21.6 nm (*16*). The protein formed very viscous solutions at a concentration of ~600 μg/mL, and concentration beyond this level by ultrafiltration on a 50 kDa membrane was extremely slow. Purified protein at 200 μg/mL (~9 μM) in phosphate buffer (pH 7.0) was incubated at room temperature for 7 days and examined by transmission electron microscopy (TEM) for formation of any fibrils. Occasionally, ~1000 nm long fibers (Figure 1) with a diameter of ~17−20 nm could be seen, but most of the protein was still in granular form. A variety of solution conditions were explored as a possible means of producing homogeneous fibrils from thioesterase at concentrations of 50 μg/mL (2.3 μM). We examined several solution conditions such as high salt concentration (5 M NaCl), low pH (2.0), 30% trifluoroethanol (TFE), and 75% ethanol in 5 mM phosphate buffer (pH 7.0). All the samples were incubated at 25 °C for 9 days. For the purposes of comparison, a solution of 50 μg/mL protein was simultaneously incubated in buffer alone at the same temperature. Aliquots of each were withdrawn at 24 h intervals to characterize amyloid formation. Fibrillar growth in 75% ethanol was found to be best and was used routinely for growing thioesterase fibrils used in this study.

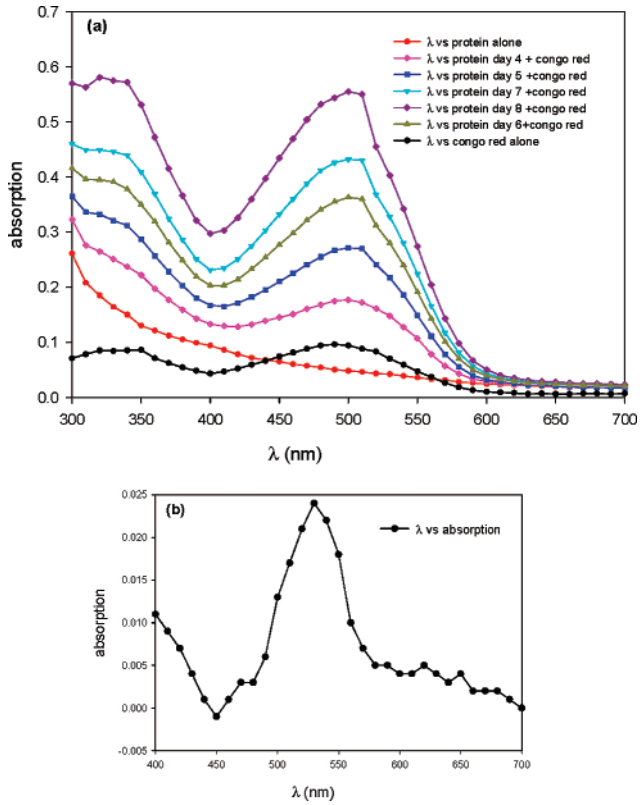

FIGURE 2: Congo red binding assay. Thioesterase was incubated in 75% ethanol at 2.3 μM, and amyloid formation was observed by measuring the increase and shift in absorbance of Congo red dye as described in Materials and Methods. (a) Samples showing an increase and shift in absorbance from 493 to 505 nm. (b) Differential spectra of the protein and dye − (dye alone + protein alone) showing absorption maxima at 535 nm. All values are means of three determinations.

Samples were tested for amyloid fibril−Congo Red (CR) binding by the spectroscopic band-shift assay (*21*). Protein sample alone in assay buffer and CR dye alone in sample buffer were used as controls. Figure 2a shows a set of typical spectra of CR before and after the addition of thioesterase fibrils. As the incubation period increased from the fifth to ninth day, dye binding is not only accompanied by a significant increase in absorption intensity but also exhibited a characteristic shift of the absorption maxima from 493 nm for CR alone to 505 nm. The point of maximal spectral difference was calculated from the differential spectrum obtained by subtracting the sum of absorption by protein alone and CR alone from the absorption spectra of a mixture of CR and protein aggregates. The differential spectra obtained from a 9-day-old sample exhibited a λ_{max} at 535 nm (Figure 2b). The λ_{max} at 520−540 nm is a characteristic feature of the amyloid fibrils (*22*, *24*). In comparison, protein samples incubated in buffer alone exhibited some increase in CR absorbance; however, there was not a characteristic shift in the absorption maxima of CR, nor did its differential spectra exhibit a λ_{max} between 520 and 540 nm. Thin films of protein samples with an alkaline CR solution were made on glass slides and observed under cross-polarized light. The protein sample incubated in 75% ethanol on the fifth day of incubation stained readily with CR, a partially dried sample of which appeared red in color and exhibited areas of green birefringence when observed under cross-polarized light (Figure 3).

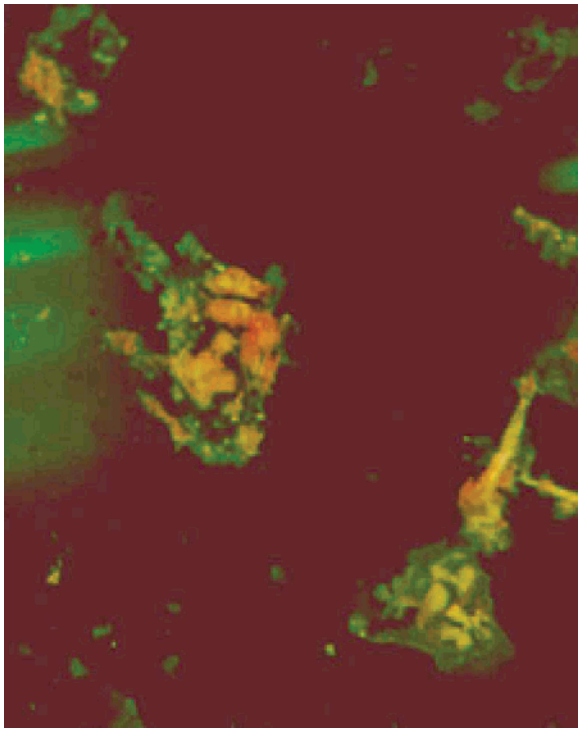

FIGURE 3: Congo red birefringence. An aliquot of sample (20 μL) was withdrawn after 5 days from the fibrillization solution (2.3 μM protein in 75% ethanol) and air-dried on a siliconized glass slide. It was stained with Congo red and visualized at 40× under a cross polarizer on an optical microscope. Green birefringence could be seen in amyloid rich areas.

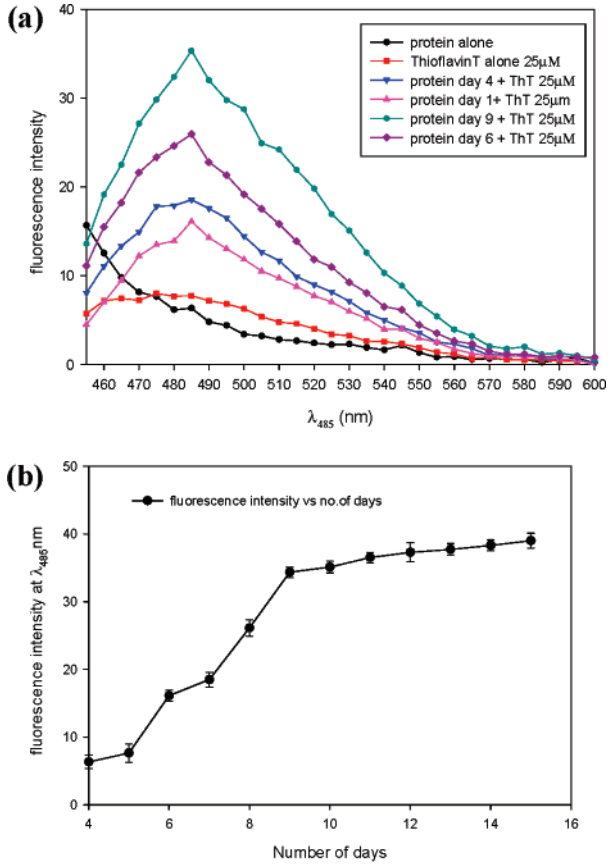

FIGURE 4: Thioflavin T binding assay. Thioesterase was incubated in 75% ethanol at 2.3 μM, and amyloid formation was observed by measuring the increase in intensity of emission spectra of the thioflavin T dye, as described in Materials and Methods. (a) Emission spectra of Thioflavin T. (b) Fluorescence intensity at 485 nm. Values are reported as the mean ± standard deviation of three experiments.

Formation of amyloids was also confirmed by a thioflavin T (ThT) binding assay. A 3−7-fold increase in the fluorescence intensity was observed depending upon the time for which protein was incubated in 75% ethanol (Figure 4). There was a sharp increase in fluorescence intensity beginning at day 4, which reached a maximum at day 9, after which it remained fairly constant. The assay was performed as described in Materials and Methods.

All the samples, which were subjected to the CR and ThT assay, were simultaneously examined by TEM in an effort to study the development and morphology of fibrils upon incubation in 75% ethanol at a concentration of 2.3 μM. Protein incubated in buffer alone at the same concentration served as a control sample. On day 2, initiation of fibril formation could be seen in induced samples (Figure 5a). On day 4, well-defined fibrils of ∼500−1000 nm with a diameter of 17−20 nm were present (Figure 5b). On day 9, the fibrils grew to more than 4000 nm, but the diameter, however, remained constant at 17−20 nm (Figure 5c). The fibrillization could also be seen in the control sample, but fibril population after 9 days remained quite low (Figure 5d) compared to those of ethanol samples.

CD spectra of samples incubated in 75% ethanol for different periods of time were obtained to determine the conformational changes that the protein may have undergone during the transition from a homogeneous population of granular aggregates to amyloid fibrils. The far-UV CD spectrum of the freshly prepared sample of protein (granulated aggregate) exhibited an intense negative ellipticity band at 218 nm, which is characteristic of β-sheet structure (Figure 6). The negative ellipiticity band at 218 nm remained constant for all the samples, incubated for various periods of time in 75% ethanol; only the intensity of the negative ellipticity band increased beginning with the 5-day-old sample. However, far-UV CD spectra of the 45-day-old sample, recorded after centrifugation at 14 000 rpm for 10 min, exhibited two negative ellipticity bands characteristic of an α-helical conformation, indicating that most of the protein has gone into fibril formation.

Effect of Seeding on Fibrillogenesis. There was a severalfold enhancement in the rate of formation of fibrils, when an aliquot of preformed fibrils was added to the freshly prepared sample of thioesterase. Thus, 50 μg/mL thioesterase was incubated in 75% ethanol for 8 days at room temperature, and 100 μL of this ethanol solution was added to a freshly prepared solution of 50 μg of thioesterase in 1 mL of 75% ethanol. The formation of fibrils was observed by CR and ThT binding assays. A significant increase in the absorption intensity of CR could be observed (Figure 7a). The absorbance of CR in the presence of a 1-day-old seeded sample was almost similar to that of a 6-day-old unseeded sample. A similar increase in the fluoresence intensity of ThT at λ_{485} was also observed for seeded samples (Figure 7b). Fourteen days after the seeding experiment, the sample was centrifuged to remove all fibrillar materials. The supernatant when observed in the far-UV region of the spectropolarimeter was found to be devoid of any structure (Figure 8). No protein could be detected in the supernatant by Bradford's method, indicating that the whole protein has

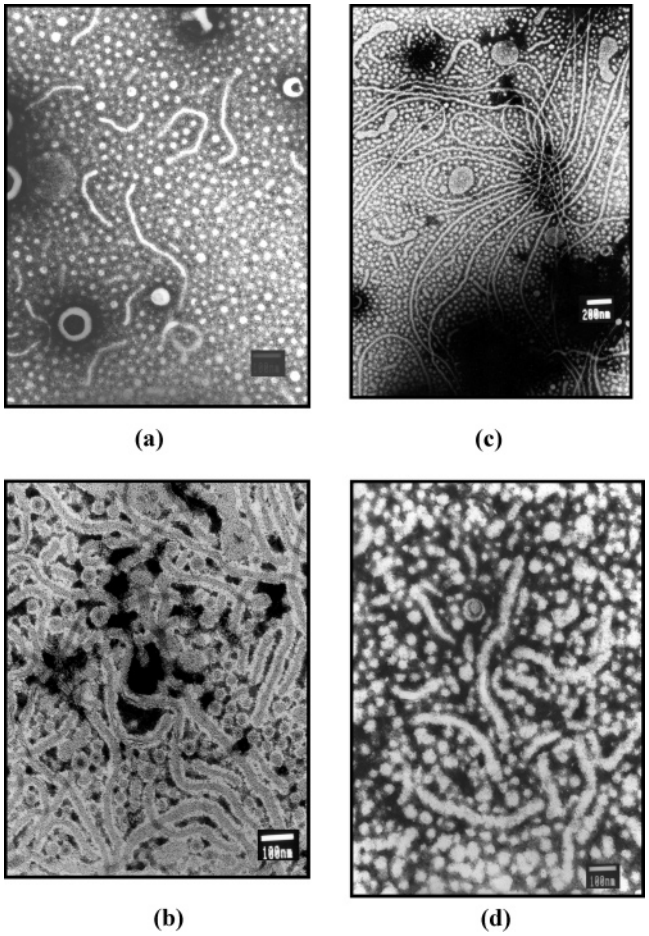

FIGURE 5: Transmission electron micrographs. Purified protein at 2.3 μM in 75% ethanol and 5 mM phosphate buffer was incubated at room temperature, and growth of fibrils was monitored by TEM: (a) 2-day-old, (b) 4-day-old, and (c) 9-day-old samples. (d) TEM of 9-day-old sample when 50 μg/mL purified protein was incubated at room temperature in buffer alone.

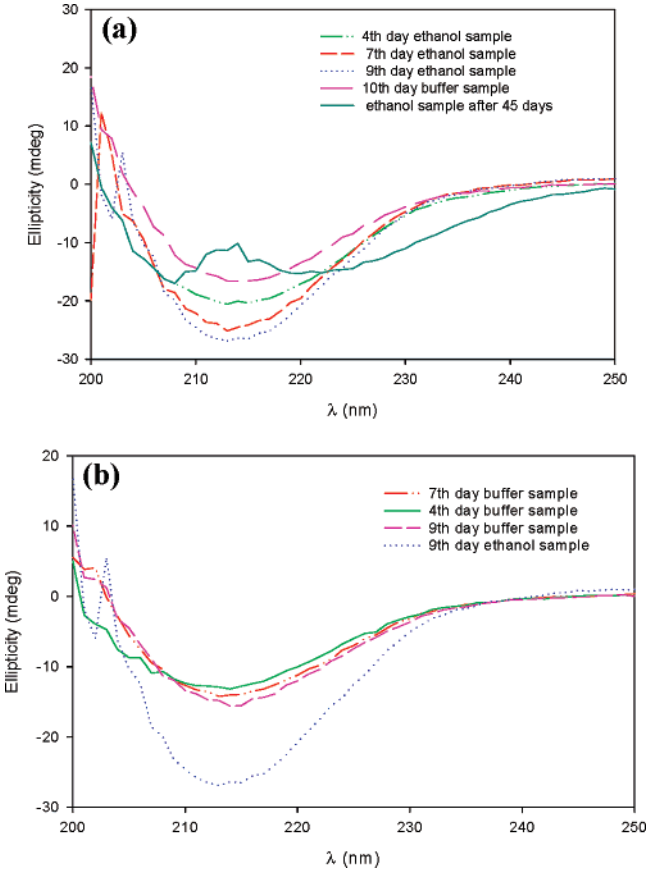

FIGURE 6: CD spectra of growing fibrils. Thioesterase incubated in 75% ethanol at 2.3 μM. Aliquots were withdrawn after particular intervals and diluted to a concentration of 2.5 μg/mL. CD spectra were recorded after centrifugation to remove aggregated material in a Jasco spectropolarimeter at room temperature in a cell with a path length of 0.1 cm. Results are expressed in terms of raw ellipticity: (a) 75% ethanol samples and (b) buffer alone (control) samples. All values are means of five determinations.

been transformed to amyloids. In comparison, the control sample, where no seeding of sample was done, showed the presence of β-oligomers after 14 days.

Mechanism of Fibrillization. TEM micrographs obtained at various stages during growth of amyloid at a protein concentration of 2.3 μM helped us to understand to a certain extent the early events in the fibrillization process. The purified protein contained oligomers as granular particles 20−25 nm in diameter (*16*). The oligomers grew to the size of ∼35−40 nm just before fusion (Figure 9b). Figure 9b shows two oligomers of 35−40 nm caught in act of fusion (marked a). Immediately after the fusion, the diameter of the resulting particle was reduced to ∼20−25 nm whereas the length increased to ∼110 nm (marked b), indicating reorganization and strengthening of the structure, which in all probability involves changes in the hydrogen bonding status. Elongation of the fiber occurred by sequential addition of oligomeric units. The length of the fiber after fusion of four units was ∼220 nm (Figure 9c). The elongation process continued to give a fiber 500−1000 nm in length with a further reduction in diameter to 17−20 nm (Figure 5b). On day 9, the fiber grew to more than 4000 nm, but the diameter remained constant at 17−20 nm (Figure 5c). No lateral fusion of units could be seen in any of the fields in electron micrographs. The periodicity of ∼35−40 nm could be clearly seen in the topography of the fibril (Figure 9e,f). This is consistent with the theory that fibrils are composed of a succession of composite units. The tendency of the fibril to form parallel sheets is quite remarkable and could be seen in fibrils grown in the presence of 75% ethanol (Figure 9f) or pH 2.0 (Figure 9d,g).

When preformed fibrils were added to a fresh solution of protein in 75% ethanol, the rate of the fibrillization process was enhanced. Figure 9h has captured (marked c) an addition of a peptide unit as an appendage to the preformed fibril. The appended peptide unit has a slightly larger diameter compared to the preformed fibril, which may have been caused by the addition of oligomeric units in rapid succession without allowing sufficient time to the appended units for reorganization and integration into the fibrils. These results clearly show that under the conditions that were used, the mature amyloid fibrils from thioesterase of *A. faecalis* are assembled via longitudinal growth of protein oligomers and not via lateral association of protofibrils.

DISCUSSION

The formation of critical size nucleus is usually the rate-determining step in amyloid fiber formation (*25*−*28*). Once these critical nuclei with the highest free energy are formed, the aggregation proceeds rapidly into amyloid fibers (*29*, *30*).

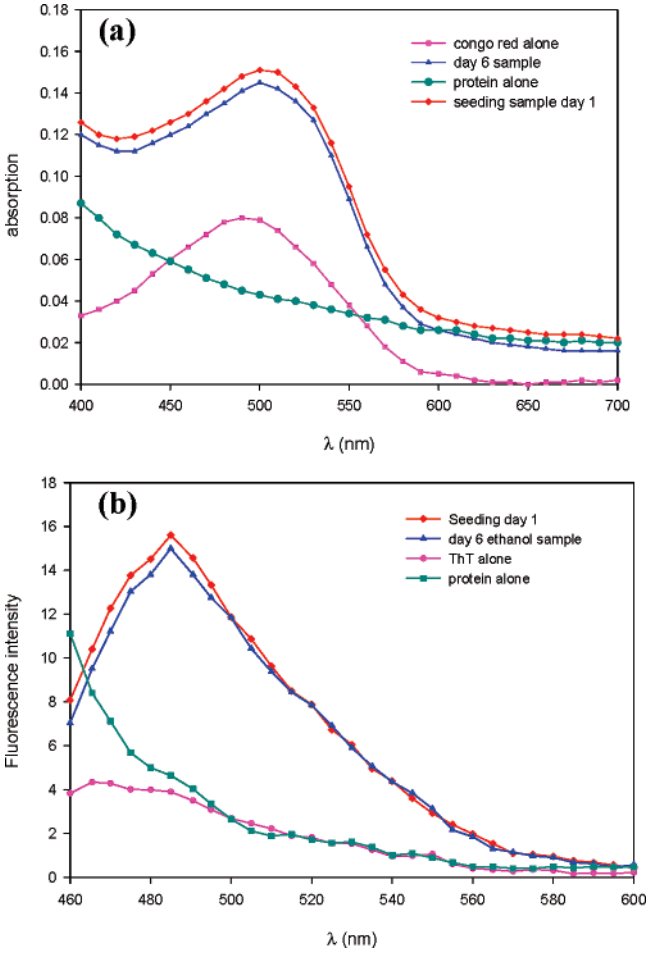

FIGURE 7: Effect of seeding on fibrillogenesis. Thioesterase was incubated in 75% ethanol at a concentration of 50 μg/mL for 8 days; 100 μL of this solution was added to a fresh solution of thioesterase (50 μg/mL) in 75% ethanol. The effect of seeding was observed by measuring the increase and shift in absorbance of Congo red (a) and by emission spectra of thioflavin T (b).

The critical size of the nucleus and also the aggregation propensity of a protein or peptide are sequence-dependent (*31*−*33*). Thermodynamically, the formation of dimer is assumed to be most unfavorable step in the process, leading to the formation of a critical size nucleus (*31*, *34*, *35*). Recent experimental data obtained during aggregation studies on tandem repeats, in which the SH3 domains of PI3 kinase were covalently linked through a flexible linker, however, did not indicate that dimer formation precedes amyloid formation (*36*).

The thioesterase of *A. faecalis* recently described by us is a constitutive, 22 kDa peripheral membrane protein (*16*, *17*). The protein was released from the cells by incubation in buffer containing 1 M sodium chloride. At a level of 600 μg, a pure sample of the protein formed very viscous solutions in buffer, which showed large granular micellelike structures 21.6 nm in average diameter when observed by TEM (*17*). The far-UV CD spectrum of the freshly prepared sample of protein (granular aggregate) exhibited an intense negative ellipticity band at 218 nm, which is characteristic of β-sheet structure. Incubation of the protein in 75% ethanol at a protein concentration of 2.3 μM resulted in the transformation of oligomers to amyloid-like fibrils, formation of which was confirmed by Congo red (Figures 2 and 3) and thioflavin T (Figure 4) binding assays and TEM (Figure 5). Alcohol is known to modify several processes such as the thermal denaturation of nucleic acids and proteins, protein folding (*37* and references cited therein), micellization of surfactant molecules (*38*), solubility of nonelectrolytes (*39*), etc. These effects have been explained on the basis of the change in solvent properties resulting from water−alcohol interactions. It is also known that at concentrations higher than 60%, molecular aggregation of alcohol molecules dominates, most likely due to the hydrophobic clustering of alkyl groups of alcohol molecules. Low-frequency Raman scattering studies show that an alcohol concentration of 60−80% (v/v) corresponds to the conditions of strongest alcohol−water interactions (*40*).

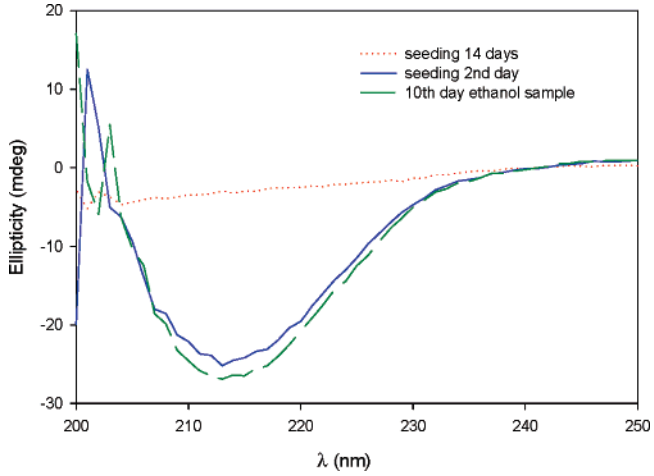

FIGURE 8: Effect of seeding on fibrillognesis. Thioesterase was incubated in 75% ethanol at 50 μg/mL for 8 days; 100 μL of this solution was added to a fresh solution of thioesterase (50 μg/mL) in 75% ethanol. Aliquots were withdrawn after particular intervals and diluted to a concentration of 2.5 μg/mL. CD spectra were recorded after centrifugation to remove aggregated material in a Jasco spectropolarimeter at room temperature in a cell with a path length of 0.1 cm. Results are expressed in terms of raw ellipticity. All values are means of five determinations.

TEM micrographs obtained at various stages during the growth of amyloid fibrils help us to understand to a certain extent the early events in the fibrillization process. The oligomers grew to a size of 35−40 nm and appeared "sticky" (Figure 9b) before two of them fused to give a higher-order structure. Immediately after fusion, the diameter of the resulting particle was reduced to 20−25 nm whereas the length increased to ∼110 nm, indicating reorganization and strengthening of the structure. The length of the fiber after fusion of four units was ∼220 nm (Figure 9c). The elongation process continued to give fibers more then 4000 nm in length; the diameter, however, was reduced further to 17−20 nm (Figure 5c). These results are consistent with the results obtained by computer simulation studies that explored the early steps of amyloid peptide aggregation, recently reported by Mousseau et al. (*31*), and may be explained as follows. Thus, once the non-native interactions bring the peptides close together, native backbone−backbone interactions start the assembly of β-sheets, but in non-native alignment of β-strands. The transition between non-native and native alignment involves a reptation move of one chain with respect to another, a mechanism that according to Mousseau et al. is independent of the size of the oligomer. The decrease in diameter accompanying the growth of oligomers observed during fibril growth of thioesterase may be explained on the

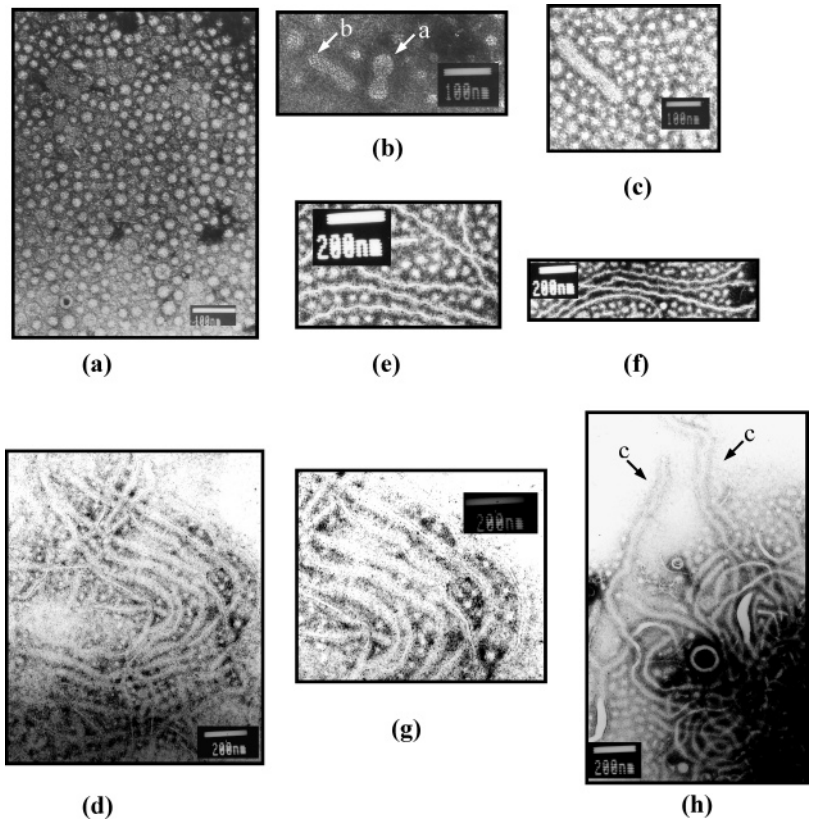

FIGURE 9: Transmission electron micrographs showing stages of fibrillar growth: (a) granular aggregates, (b) two oligomers caught in the act during fusion, (c) fibril corresponding to four oligomers, (d) fibrils formed at pH 2.0, (e) topography of fibril showing the periodicity, (f and g) parallel organization of fibrils in 75% ethanol and at pH 2.0, respectively, and (h) topography of fibrils formed upon seeding with preformed fibrils.

basis of this reorganization of structure, which brings about the transition between off-registry and in-registry β-sheets. These non-native β-sheets are thought to represent kinetic traps, which contribute to the lag phase period. The reorganization of β-strands within the oligomer appears to be driven by native side chain−side chain interactions. Finally, the repacking of the side chains within the reduced volume that occurs due to the reduction in diameter of the growing particle would force the β-sheets to be separated by a slightly longer distance, thus leading to the elongation of the oligomer.

A hierarchical two-stage model has been revoked recently to account for the results of aggregation studies of the SH3 domain of phosphatidylinositol 3′-kinase (PI3-SH3) at low pH (<3.0) (*36*). In this mechanism, called "nucleated conformation conversion", the protein initially segregated between the soluble phase and the dispersed phase of oligomeric intermediates as a result of spinodal decomposition (*41*, *42*). The dispersed phase aggregates are thought to be fluidlike species described as "molten oligomers" perhaps with micellelike features (*28*, *41*). Structural reorganization of these intermediates leads to the formation of small amyloid-like structures, which triggers rapid growth of fibrils. Accordingly, the formation of a critical nucleus from the SH3 domain under low-pH conditions and its subsequent growth to amyloid fibers were explained as follows (*36*). Although at low pH the molecules of the SH3 domain carry a net positive charge and are soluble, it was suggested that a fraction of molecules is transiently populated at neutral charge, which spontaneously aggregate by an energetically favorable colloid coagulation reaction. The hypothesis was based on observation that spontaneous aggregation of SH3 domain molecules occurred at pH 3.6, which is close to the isoelectric point of the protein and where the molecules were expected to carry a net charge close to zero. Once sufficient molecules are present within the oligomer, reorganization steps become thermodynamically favorable as a result of an increase in the number of hydrogen bonds and other stabilizing interactions. Once fragments of highly ordered aggregates are present, the free energy for addition of monomeric molecules to a growing fibril becomes more favorable. Thioesterase used in this study exists as soluble oligomers 21.6 nm in diameter in buffer. A further increase in the size of the oligomer occurs very slowly, as under these solution conditions the protein molecules apparently have already been successful in hiding most of their hydrophobic surfaces. When the solution conditions were perturbed by addition of 75% ethanol, coalescence of two initially formed spherical oligomeric structures occurred, resulting in the formation of larger spherical particles. In the next step, coalescence of two of these larger size oligomers occurred with concomitant reorganization of the structure leading to a reduction in diameter and an increase in length, i.e., formation of a small amyloid-like structure (protofibrils). These steps are sometimes termed side-by-side (lateral) association of oligomers (*31*, *43*). Thus, the first stage in the hierarchical two-stage model, the formation of the critical size nucleus in the case of thioesterase, may be considered to be composed of two steps, spontaneous formation of intermediate size soluble oligomers and their coalescence to generate higher-order structures, both steps being dependent on solution conditions.

In the hierarchical two-stage model, the second stage in the assembly process requires addition of denatured soluble monomeric molecules to the growing fibril (*36*). However, the results reported herein for thioesterase suggest that further growth of fibrils in the second stage occurs by the longitudinal addition of full-sized oligomers and not by addition of monomers. The diameter of oligomers was reduced at the initial stages of fiber growth, suggesting that under the conditions that were used, the mature fibers of thioesterase are assembled via longitudinal growth of oligomers and not via lateral growth of protofibrils. However, the aggregation of proteins is a complex process and depends on several parameters, such as amino acid constitution and sequence and solution conditions (*31*−*33*). In addition, the same protein may follow multiple mechanisms of aggregation, depending on the conditions that are used; for example, aggregation of PI3-SH3 take place by a variety of mechanisms, ranging from downhill formation of relatively amorphous species to nucleated formation of highly organized structures, the relative importance of which varies greatly with solution conditions (*36*). Therefore, the process observed for thioesterase may not be a general process, especially in light of the earlier studies where protofibril has been proposed as a building block of the thicker higher-order mature fibrils, which were thought to form by lateral association of protofibrils (*11*, *14*).

This study and those reported elsewhere indicate that the growth of amyloids to either the soluble oligomers or mature fibrils strongly depends on the solution conditions (*44* and references cited therein). A large volume of recent experimental data derived from disease-related and disease-unrelated proteins suggest that amyloid species toxic to cells are prefibrillar aggregates rather than mature fibrils (reviewed in ref *1*). However, a recent study has shown that overt neuronal cell death mediated by Aβ1−40 was critically dependent on ongoing Aβ1−40 nucleation-dependent polymerization, which in turn was dependent on the concentration of both soluble oligomers and fibrillar Aβ (*18*). Neither amyloid fibrils alone nor soluble oligomers of Aβ alone were able to cause overt neuronal cell death. A close relationship was shown to exist between the rate of Aβ polymerization and both the rate and extent of Aβ-mediated neuronal cell death. The neurotoxic potency of Aβ increased as the number of fibril ends increased, as would be expected for a nucleation-dependent polymerization process. This is consistent with the observation that in nucleation-dependent polymerization, the seeding efficiency depends on the number of fiber ends and not on the lateral surface of the fiber (*29*, *41*). The results of seeding experiments obtained during amyloid growth of thioesterase become significant when viewed in the context of the forgoing discussion. When preformed fibrils were added to a fresh solution of protein in 75% ethanol, the rate of fibrillization was enhanced, which clearly indicates that fibril growth is dominated by a nucleation mechanism. Figure 9h shows an addition of a peptide unit as an appendage to the preformed fibril. The appended peptide unit has a diameter slightly larger than that of the preformed fibril, which might have happened because of the addition of oligomeric units in rapid succession without the allowance of sufficient time to the appended units for reorganization and integration into the fibrils. These data suggest that although the lateral surface of the fiber is quite inert as no lateral fusion could be seen, the fiber end appears quite reactive and is able to bring about requisite conformational changes in oligomeric units of proteins to make them fusogenic. The effect appears to happen in a cascade, and the added unit even before its own integration with the growing fibril induces fusogenicity in the next oligomeric unit.

It is becoming increasingly apparent that the ability to form amyloid structures is not an unusual feature of the small number of disease-related proteins but appears to be a generic property of peptides and proteins. A number of studies have been reported in which full-length proteins, unrelated to any known amyloid disease, aggregated in vitro to form structures indistinguishable from the amyloid fibrils obtained from disease-related proteins (*1*, *5*−*7*). In each case, aggregation of proteins to form amyloid fibrils required solution conditions which caused the native structure to be partially disrupted, but interactions such as hydrogen bonding were not completely disrupted. Thioesterase of *A. faecalis* may be regarded as the latest addition to the growing list of such disease-unrelated amyloid-forming proteins. Although ethyl alcohol is not a physiological solvent, its use in these studies does point to the general solution conditions for growth of amyloids from proteins. As stated above, several studies have shown that the effects due to alcohol on very different systems and processes such as the thermal denaturation of nucleic acids and proteins, protein folding, micellization of surfactant molecules, or the solubility of nonelectrolytes are strikingly similar (*37*−*39*). It is generally believed that the observed effects are not due to binding of alcohol molecules to functional groups of macromolecules but to a indirect mechanism in which changes in solvent properties result from the addition of alcohol. The change in solvent properties may result from incomplete mixing at the molecular level as suggested recently rather than a change in water structure proposed earlier and can be associated with hydrophobic clustering of alkyl groups of alcohol molecules (*45*). Similar solution conditions may occur in vivo, especially in free or esterified cholesterol rich regions. Results of a recent study on autopsied brain tissue from Alzheimer's disease (AD) patients after immunochemistry with a monoclonal antibody that recognized Aβ peptides are of particular interest in this connection. AD samples exhibited both more positive neurons and more stained reaction product per neuron compared to non-AD samples. Ultrastructurally, the immunopositive reaction product accumulated in clusters of cytoplasmic elements that were closely apposed to lipid droplets (*46*).

ACKNOWLEDGMENT

We acknowledge the help provided by Dr. Manoj Raje in EM studies.

REFERENCES

1. Stefani, M., and Dobson, C. M. (2003) Protein aggregation and aggregate toxicity: New insights into protein folding, misfolding diseases and biological evolution, *J. Mol. Med. 81*, 678−699.
2. Ehud, G. (2005) Mechanisms of amyloid fibril self-assembly and inhibition by model short peptides as a key research tool, *FEBS J. 272*, 5971−5978.
3. Rochet, J. C., and Lansbury, P. T., Jr. (2000) Amyloid fibrillogenesis: Themes and variations, *Curr. Opin. Struct. Biol. 10*, 60−68.

4. Serpell, L. C. (2000) Alzheimer's amyloid fibrils: Structure and assembly, *Biochim. Biophys. Acta 1502*, 16−30.
5. Guijarro, J. I., Sunde, M., Jones, J. A., Campbell, I. D., and Dobson, C. M. (1998) Amyloid fibril formation by an SH3 domain, *Proc. Natl. Acad. Sci. U.S.A. 95*, 4224−4228.
6. Gross, M., Wilkins, D. K., Pitkeathly, M. C., Chung, E. W., Higham, C., Clark, A., and Dobson, C. M. (1999) Formation of amyloid fibrils by peptides derived from the bacterial cold shock protein CspB, *Protein Sci. 8*, 1350−1357.
7. Litvinovich, S. V., Brew, S. A., Aota, S., Akiyama, S. K., Haudenschild, C., and Ingham, K. C. (1998) Formation of amyloid-like fibrils by self-association of a partially unfolded fibronectin type III module, *J. Mol. Biol. 280*, 245−258.
8. Chapman, M. R., Robinson, L. S., Pinkner, J. S., Roth, R., Heuser, J., Hammar, M., Normark, S., and Hultgren, S. J. (2002) Role of *Escherichia coli* curli operons in directing amyloid fiber formation, *Science 295*, 851−855.
9. Claessen, D., Rink, R., de Jong, W., Siebring, J., de Vreugd, P., Boersma, F. G., Dijkhuizen, L., and Wosten, H. A. (2003) A novel class of secreted hydrophobic proteins is involved in aerial hyphae formation in *Streptomyces coelicolor* by forming amyloid-like fibrils, *Genes Dev. 17*, 1714−1726.
10. Gebbink, M. F., Claessen, D., Bouma, B., Dijkhuizen, L., and Wosten, H. A. (2005) Amyloids: A functional coat for microorganisms, *Nat. Rev. Microbiol. 3*, 333−341.
11. Goldsbury, C. S., Cooper, G. J., Goldie, K. N., Muller, S. A., Saafi, E. L., Gruijters, W. T., Misur, M. P., Engel, A., Aebi, U., and Kistler, J. (1997) Polymorphic fibrillar assembly of human amylin, *J. Struct. Biol. 119*, 17−27.
12. Harper, J. D., Wong, S. S., Lieber, C. M., and Lansbury, P. T. (1997) Observation of metastable Aβ amyloid protofibrils by atomic force microscopy, *Chem. Biol. 4*, 119−125.
13. Walsh, D. M., Hartley, D. M., Kusumoto, Y., Fezoui, Y., Condron, M. M., Lomakin, A., Benedek, G. B., Selkoe, D. J., and Teplow, D. B. (1999) Amyloid β-protein fibrillogenesis. Structure and biological activity of protofibrillar intermediates, *J. Biol. Chem. 274*, 25945−25952.
14. Goldsbury, C., Kistler, J., Aebi, U., Arvinte, T., and Cooper, G. J. (1999) Watching amyloid fibrils grow by time-lapse atomic force microscopy, *J. Mol. Biol. 285*, 33−39.
15. Green, J. D., Goldsbury, C., Kistler, J., Cooper, G. J., and Aebi, U. (2004) Human amylin oligomer growth and fibril elongation define two distinct phases in amyloid formation, *J. Biol. Chem. 279*, 12206−12212.
16. Shahi, P., Kumar, I., Sharma, R., Sangar, S., and Jolly, R. S. (2006) Characterization of a novel long-chain acyl-coA thioesterase from *Alcaligenes faecalis*, *FEBS J. 273*, 2374−2387.
17. Kumar, I., and Jolly, R. S. (2001) A thioesterase for chemoselective hydrolysis of S-acyl sulfanylalkanoates, *Org. Lett. 3*, 283−285.
18. Wogulis, M., Wright, S., Cunningham, D., Chilcote, T., Powell, K., and Rydel, R. E. (2005) Nucleation-Dependent Polymerization Is an Essential Component of Amyloid-Mediated Neuronal Cell Death, *J. Neurosci. 25*, 1071−1080.
19. Bucciantini, M., Giannoni, E., Chiti, F., Baroni, F., Formigli, L., Zurdo, J., Taddei, N., Ramponi, G., Dobson, C. M., and Stefani, M. (2002) Inherent toxicity of aggregates implies a common mechanism for protein misfolding diseases, *Nature 416*, 507−511.
20. Barnes, E. M., Jr., and Wakil, S. J. **(**1968) Studies on the mechanism of fatty acid synthesis. XIX. Preparation and general properties of palmitoyl thioesterase, *J. Biol. Chem. 243*, 2955−2962.
21. Klunk, W. E., Jacob, R. F., and Mason, R. P. (1999) Quantifying amyloid by congo red spectral shift assay, *Methods Enzymol. 309*, 285−305.
22. Klunk, W. E., Pettegrew, J. W., and Abraham, D. J. (1989) Quantitative evaluation of congo red binding to amyloid-like proteins with a β-pleated sheet conformation, *J. Histochem. Cytochem. 37*, 1273−1281.
23. LeVine, H., III (1995) Thioflavin T interaction with amyloid β sheet structure, *Amyloid: Int. J. Exp. Clin. Invest. 2*, 1−6.
24. Chiti, F., Bucciantini, M., Capanni, C., Taddei, N., Dobson, C. M., and Stefani, M. (2001) Solution conditions can promote formation of either amyloid protofilaments or mature fibrils from the HypF N-terminal domain, *Protein Sci. 10*, 2541−2547.
25. Kelly, J. W. (1998) The alternative conformations of amyloidogenic proteins and their multi-step assembly pathways, *Curr. Opin. Struct. Biol. 8*, 101−106.
26. Jarret, J. T., and Lansbury, P. T., Jr. (1993) Seeding the one-dimensional crystallization of amyloid: A pathogenic mechanism in Alzheimer's disease and scrapie? *Cell 73*, 1055−1058.
27. Soreghan, B. J. K., and Glabe, C. (1994) Surfactant properties of Alzheimer's Aβ peptides and the mechanism of amyloid aggregation, *J. Biol. Chem. 269*, 28551−28554.
28. Lomakin, A., Chung, D. S., Benedek, G. B., Kirschner, D. A., and Teplow, D. B. (1996) On the nucleation and growth of amyloid β-protein fibrils: Detection of nuclei and quantitation of rate constants, *Proc. Natl. Acad. Sci. U.S.A. 93*, 1125−1129.
29. Harper, J. D., and Lansbury, P. T., Jr. (1997) Models of amyloid seeding in Alzheimer's disease and scrapie: Mechanistic truths and physiological consequences of the time-dependent solubility of amyloid proteins, *Annu. Rev. Biochem. 66*, 385−407.
30. Bitan, G., and Teplow, D. B. (2004) Rapid photochemical cross-linking: A new tool for studies of metastable, amyloidogenic protein assemblies, *Acc. Chem. Res. 37*, 357−364.
31. Mousseau, M., and Derreumaux, P. (2005) Exploring the Early Steps of Amyloid Peptide Aggregation by Computers, *Acc. Chem. Res. 38*, 885−891.
32. Cecchini, M., Curcio, R., Pappalardo, M., Melki, R., and Caflisch, A. (2006) A Molecular Dynamics Approach to the Structural Characterization of Amyloid Aggregation, *J. Mol. Biol. 357*, 1306−1321.
33. Lopez de la Paz, M., and Serrano, L. (2004) Sequence determinants of amyloid fibril formation, *Proc. Natl. Acad. Sci. U.S.A. 101*, 87−92.
34. Eigen, M. (1996) Prionics or the kinetic basis of prion diseases, *Biophys. Chem. 63*, A1−A18.
35. Durbin, S. D., and Feher, G. (1996) Protein crystallization, *Annu. Rev. Phys. Chem. 47*, 171−204.
36. Bader, R., Bamford, R., Zurdo, J., Luisi, B. F., and Dobson, C. M. (2006) Probing the mechanism of amyloidogenesis through a tandem repeat of the PI3-SH3 domain suggests a generic model for protein aggregation and fibril formation, *J. Mol. Biol. 356*, 189−208.
37. Cinelli, S., Onori, G., and Santucci, A. (1999) Effect of 1-alcohols on micelle formation and protein folding, *Colloids Surf., A 160*, 3−8.
38. Ruiz-Pena, M., Comas-Rojas, H., Rodriguez-Calvo, S., and Perez-Gramatges, A. (2005) Self-association behaviour of protein: surfactant systems in alcohol/water mixtures, *Nanobiotechnol., IEEE Proc. 152*, 177−181.
39. Krzaczkowska, J., Gierszewski, J., and Slosarek, G. (2004) Solubility of adenine and kinetin in water−ethanol solutions, *J. Solution Chem. 33*, 395−340.
40. Amo, Y., and Tominaga, Y. (2000) Low-frequency Raman study of ethanol-water mixture, *Chem. Phys. Lett. 320*, 703.
41. Serio, T. R., Cashikar, A. G., Kowal, A. S., Sawicki, G. J., Moslehi, J. J., Serpell, L., et al. (2000) Nucleated conformational conversion and the replication of conformational information by a prion determinant, *Science 289*, 1317−1321.
42. San Biagio, P. L., Martorana, V., Emanuele, A., Vaiana, S. M., Manno, M., Bulone, D., et al. (1999) Interacting processes in protein coagulation, *Proteins: Struct., Funct., Genet. 37*, 116−120.
43. Gregoire, C., Marco, S., Thimonier, J., Duplan, L., Laurine, E., Chauvin, J.-P., Michel, B., Peyrot, V., and Verdier, J.-M. (2001) Three dimensional structure of the lithostathine protofilament, a protein involved in Alzheimer's disease, *EMBO J. 20*, 3313−3321.
44. Chiti, F., Bucciantini, M., Capanni, C., Taddei, N., Dobson, C. M., and Stefani, M. (2001) Solution conditions can promote formation of either amyloid protofilaments or mature fibrils from the HypF N-terminal domain, *Protein Sci. 10*, 2541−2547.
45. Dixit, S., Crain, J., Poon, W. C. K., Finney, J. L., and Soper, A. K. (2002) Molecular segregation observed in a concentrated alcohol−water solution, *Nature 416*, 829−831.
46. Gómez-Ramos, P., and Morán, M. A. (2007) Ultrastructural localization of intraneuronal Aβ-peptide in alzheimer disease brains, *J. Alzheimer's Dis. 11*, 53−59.

BI7001136